Supporting Information

Lasing from Lead Halide Perovskite Semiconductor Microcavity System

Jun Wang[1], Peimei Da[2], Zhe Zhang[1], Song Luo [1], Liming Liao[1], Zeyuan Sun[1], Xuechu Shen[1], Shiwei Wu[1], Gengfeng Zheng[2], Zhanghai Chen[1*]

*Corresponding author Email: zhanghai@fudan.edu.cn

1. Analysis of the Exciton binding energy (EBE) from absorption spectra

We have deduced EBE of $CH_3NH_3PbI_3$ from the absorption measurement, as shown as Figure S1. Figure S1a and S1b show the fittings of the exciton peak (red dashed line), the band edge absorption (blue dashed dot line) and the deduced EBE (yellow area) from the absorption spectra for the thin film of $CH_3NH_3PbI_3$. We have fitted the absorption spectra at 15K to 90K, by the framework of the Elliot's theory of Wannier excitons expressed as:

$$\alpha(\hbar\omega) \propto \frac{\mu_{cv}^2}{\hbar\omega} \sum_j |\varphi_j(r=0)|^2 \delta(\hbar\omega - E_j) \propto \frac{\mu_{cv}^2}{\hbar\omega}$$

$$\left[\sum_j \frac{4\pi\sqrt{E_b^3}}{j^3} \delta(\hbar\omega - E_j^b) + \frac{2\pi\sqrt{E_b}\theta(\hbar\omega - E_g)}{1 - e^{-2\pi\sqrt{\frac{E_b}{\hbar\omega - E_g}}}} \right]$$

Where μ_{cv} is the transition dipole moment; $\hbar\omega$ is the photon energy; $\alpha(\hbar\omega)$ is proportional to the weighted density of electron–hole pair states, with the weight provided by the probability for an electron and a hole to be at the same position $|\varphi_j(r=0)|^2$, where φ_j represents the exciton wavefunction of bound and unbound states. Bound states with energy is $E_j^b = E_g - \frac{E_b}{j^2}$; the bandgap is E_g; $\delta(x)$ and $\theta(x)$ are the Dirac-delta and the Heaviside step functions, respectively. In Figure S1a and S1b, we can obtain the EBE of 24meV and 25meV at 30K and 40K, respectively, calculated by the difference between the fitted exciton peak (755 nm at 30K and 751 nm at 40K) and band edge absorption (744 nm at 30K and 739 nm at 40K). These values can defense the thermal energy $k_b T$ for demonstrating the excitonic lasing in our sample. Moreover, we have calculated and compared the EBEs at 15K to 90K, as shown as Figure S1c, indicating the EBE ranges about from 25meV to 30meV and agreeing with the pervious reports[3]. With the temperature increasing, we can observe the exciton absorption peak has a blueshift in orthorhombic phase of $CH_3NH_3PbI_3$.

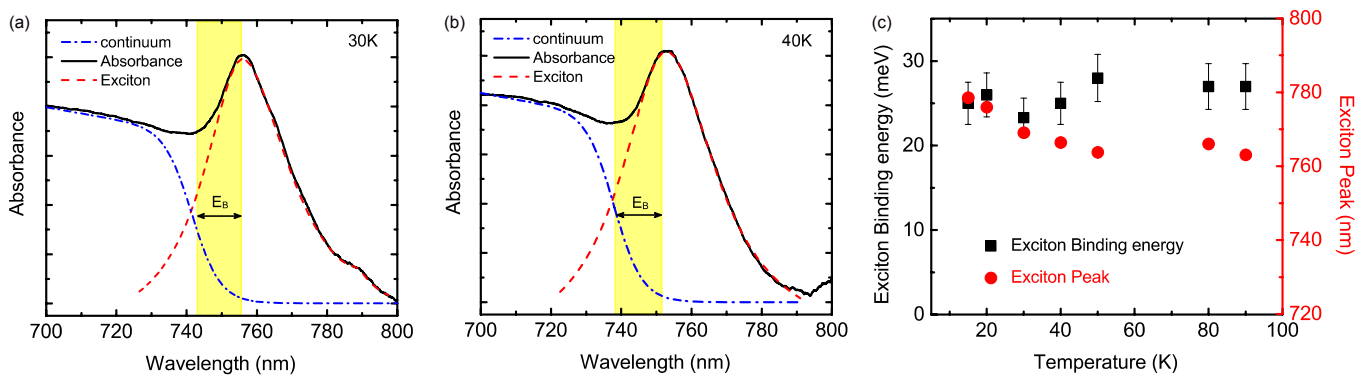Figure S1. Analysis of the experimental absorption spectra for $CH_3NH_3PbI_3$ films. (a)-(b) Absorption spectra computed according to Elliott formula. The black lines are the absorption spectrum, the red dashed lines are exciton peaks (755 nm at 30K and 751 nm at 40K), the blue dashed dot lines is the band edge absorption (744 nm at 30K and 739 nm at 40K), and the yellow area is the deduced EBE. (c) Exciton binding energy versus temperature (black squares) and Exciton peak position versus temperature (red circles), extracted from absorption spectra with Elliott formula.

2. Laser characteristics for multi-mode cavity at 30K

To verity FP-mode lasing, we have carried out experiments about angle-resolved PL below and above lasing threshold at 30K, for the case of multi-mode cavity, as shown as Figure S2. The left and right panel of Figure S2a show angle-resolved PL below and above lasing threshold for the multi-mode case, respectively. Below threshold, we can see the exciton PL emission splits into multiple peaks in the linear regime, with unequal energy difference and flat dispersions, due to some local defects on the uneven surface of metal-perovskite-DBR hybrid cavity. Above threshold, the most optimized mode is selected for the FP mode oscillation lasing. The SE peak narrow to become a lasing peak with linewidth of 0.2 nm (inset of Figure S2b), and the lasing emission displays a high coherence in every direction of k-space, as a point light source. Figure S2b show that the output PL intensity versus pump fluence, indicating the PL intensity is enhanced nonlinearly above threshold.
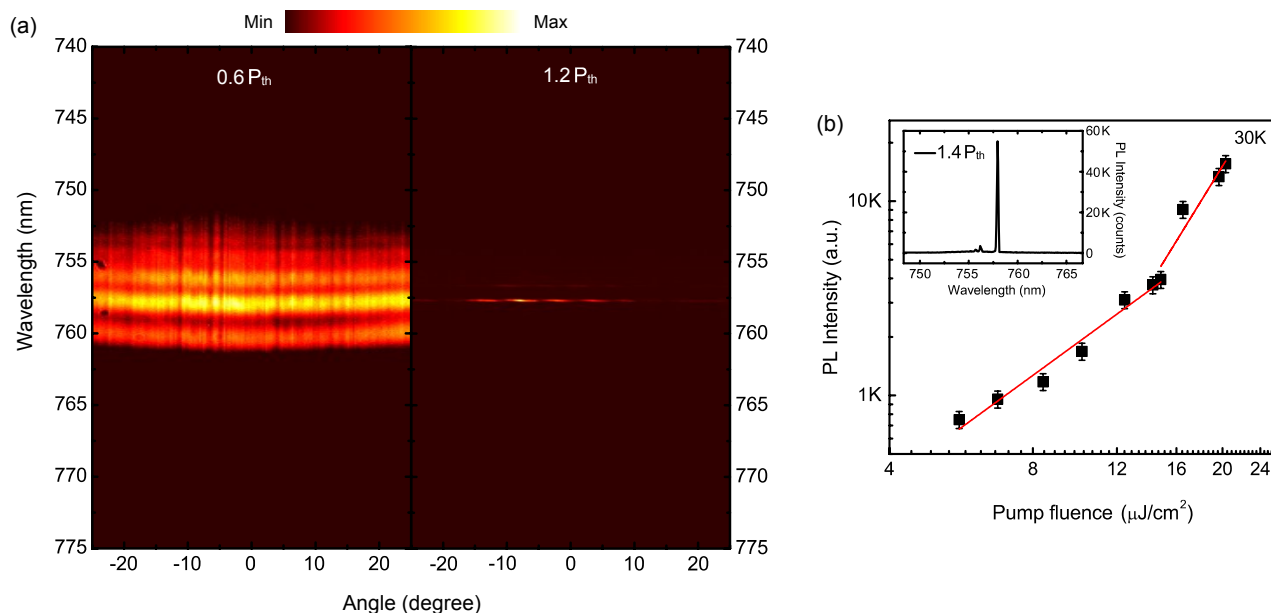

Figure S2. Laser characteristics for multi-mode cavity at 30K. (a) Angle-resolved PL spectra. Left: below threshold ($0.6 P_{th}$), right: above threshold ($1.2 P_{th}$). Angle represents the detection angle. (b) Laser output versus pump fluence, showing the

threshold is 12.9 μJ/cm^2. The inset is the PL spectrum above threshold ($1.4^{P}{}_{th}$), and the linewidth is 0.2 nm.

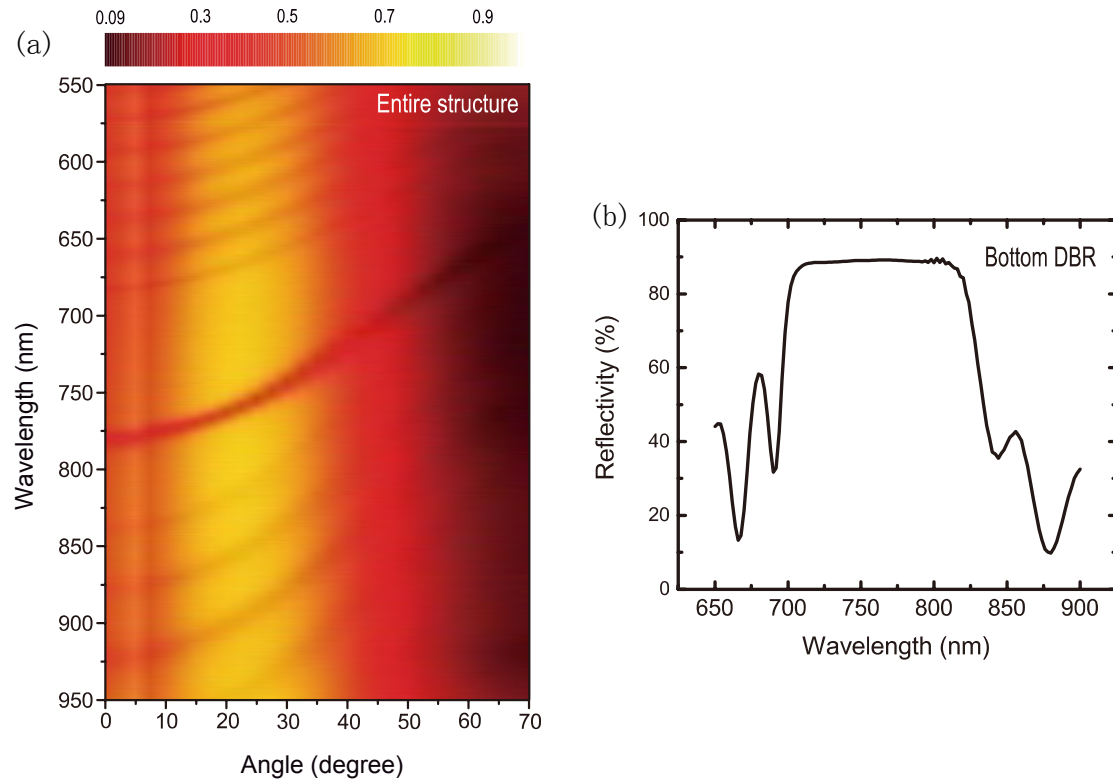## 3. Lasing characterizations at different low temperatures

Figure S3: (a) The image represents the angle-resolved reflectivity spectral mapping of the PM system at room temperature. The angle is the detection angle. The reflectivity dispersion obeys the rule of optical bandgap for one dimensional photon crystal, also modulated by the angle. (b) The reflectivity stopband of the bottom DBR mirror at normal detection ranges from 700 nm to 820nm, and its reflectivity rate reaches to the maximum about 90% at 760 nm.
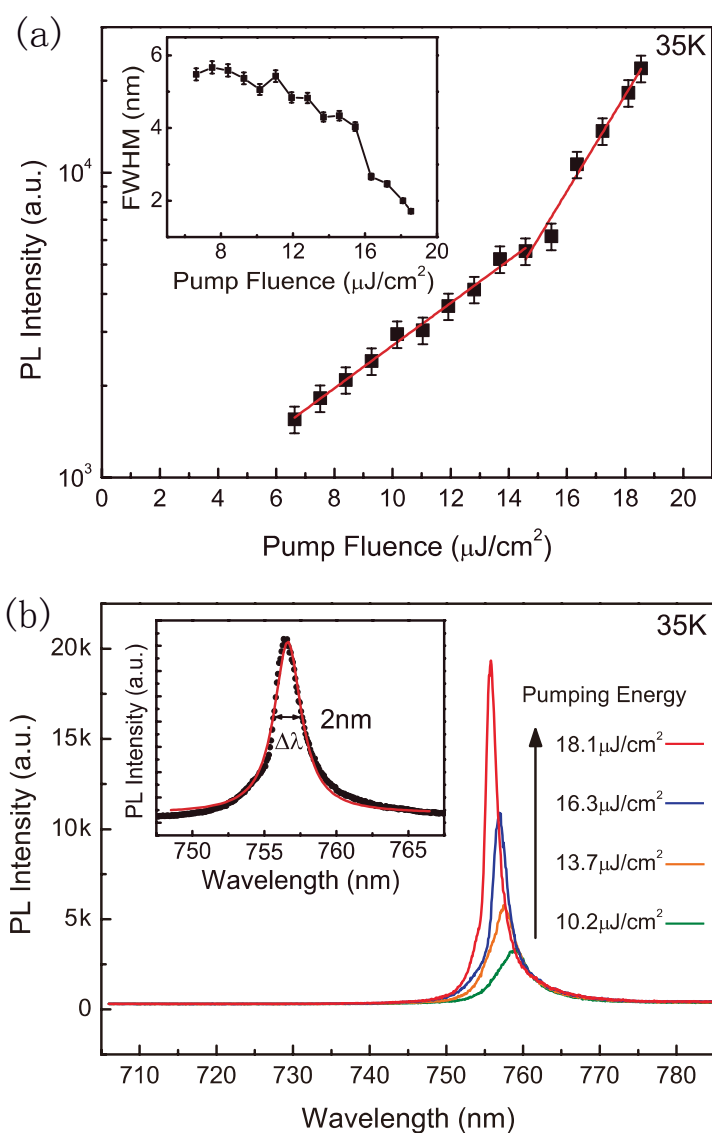
Figure S4: (a) Nonlinear response for the laser output intensity versus the pump fluence at 35 K, showing the lasing action and this threshold is 14.6 μJ cm^{-2}. The inset is the relevant full width at half maximum (FWHM) of PL peak versus pump fluence, indicating the PL peaks linewidth narrow down above this threshold. (b) The PL spectra with pumping power increase at 35 K. The pumping power of curves from bottom to up is 10.2, 13.7, 16.3 and 18.1 μJ cm^{-2}, respectively. A series of PL peaks show a blueshift when pumping power increase. The inset is a Lorentz fitting of a lasing mode (18.1 μJ cm^{-2}), and the FWHM of this mode is 2 nm at 755.8 nm. The slight asymmetric profile for the PL of figure S2(b) is likely due to background subtraction.
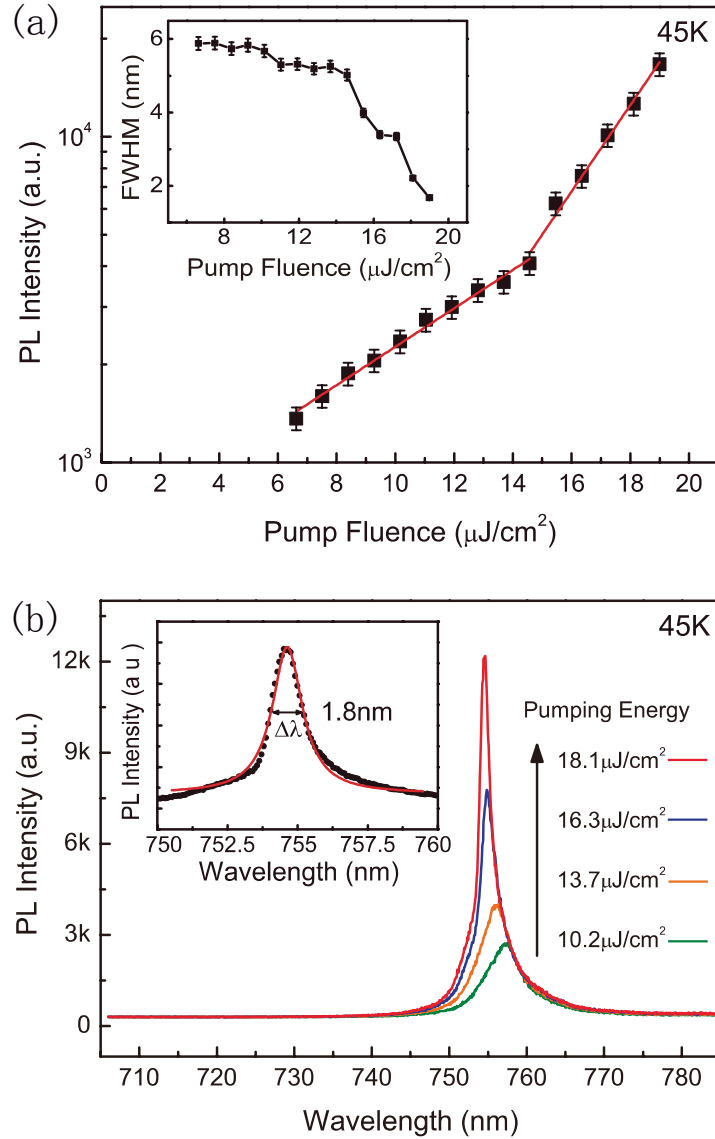
Figure S5: (a) Nonlinear response for the laser output intensity versus the pump fluence at 45 K, showing the lasing action and this threshold is 15 μJ cm^{-2}. The inset is the relevant FWHM of PL peak versus pump fluence, indicating the PL peaks linewidth narrow down above this threshold. (b) The PL spectra with pumping power increase at 45 K. The pumping power of curves from bottom to up is 10.2, 13.7, 16.3 and 18.1 μJ cm^{-2}, respectively. A series of PL peaks show a blueshift when pumping power increase. The inset is a Lorentz fitting of a lasing mode (18.1 μJ cm^{-2}), and the FWHM of this mode is 1.8 nm at 754.6 nm. The slight asymmetric profile for the PL of figure S3(b) is likely due to background subtraction.
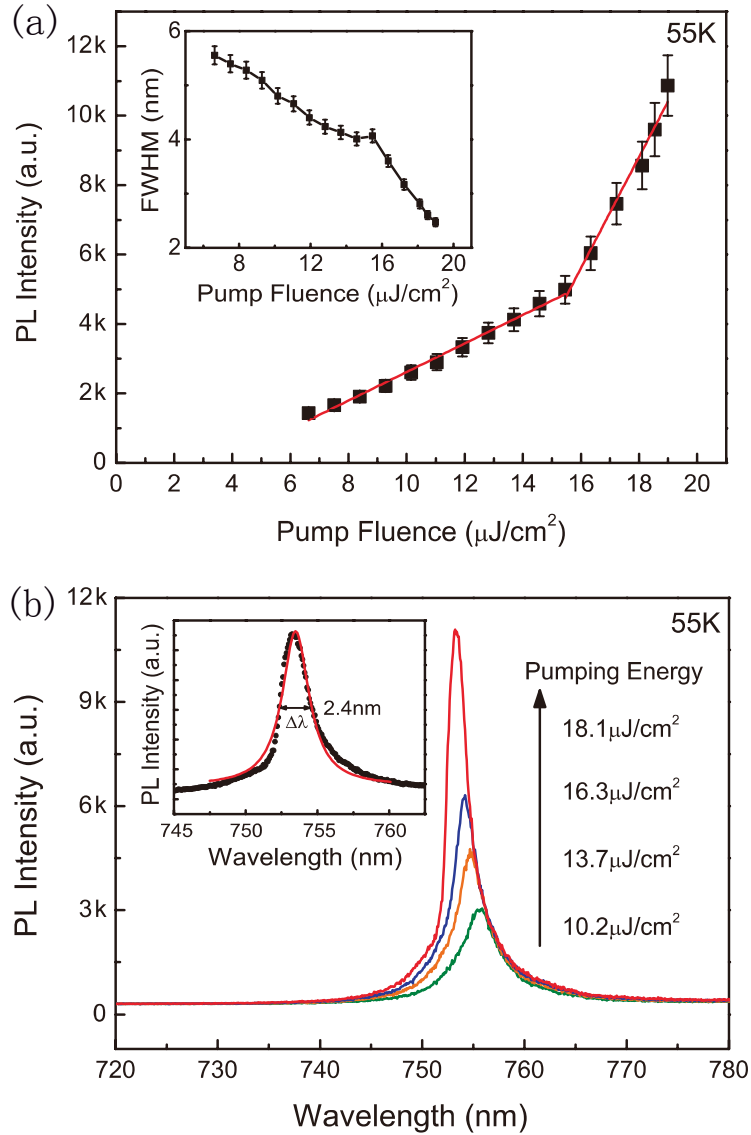
Figure S6: (a) Nonlinear response for the laser output intensity versus the pump fluence at 55 K, showing the lasing action and this threshold is 15.6 μJ cm^{-2}. The inset is the relevant FWHM of PL peak versus pump fluence, indicating the PL peaks linewidth narrow down above this threshold. (b) The PL spectra with pumping power increase at 55 K. The pumping power of curves from bottom to up is 10.2, 13.7, 16.3 and 18.1 μJ cm^{-2}, respectively. A series of PL peaks show a blueshift when pumping power increase. The inset is a Lorentz fitting of a lasing mode (18.1 μJ cm^{-2}), and the FWHM of this mode is 2.4 nm at 753.2 nm. The slight asymmetric profile for the PL of figure S4(b) is likely due to background subtraction.